

# Observation of white-light amplified spontaneous emission from carbon nanodots under laser excitation

Wen Fei Zhang, Li Bin Tang, Siu Fung Yu,\* and Shu Ping Lau

Department of Applied Physics, The Hong Kong Polytechnic University, Hung Hom, Kowloon, Hong Kong  
\*sfyu21@hotmail.com

**Abstract:** A conventional laser irradiation method is applied to fabricate carbon nanodots (C-dots). By uniformly dispersing the C-dots into N-Methylpyrrolidone (NMP) solution, white-light amplified spontaneous emission can be observed from the mixture under laser excitation at 266 nm. Peak wavelength and linewidth of the emission spectra are found to be around 450 and 120 nm respectively. It is verified that the presence of NMP enhances the emission efficiency of C-dots over the broad emission spectrum. This is because the excitation energy, which is not absorbed by the C-dots, is captured by the NMP and is subsequently transferred to the C-dots. Optical gain per peak power of the mixture at ~450 nm is found to be  $\sim 64 \text{ cm}^{-1} \text{ MW}^{-1}$ , which is about 39% higher than that without the use of NMP.

©2012 Optical Society of America

**OCIS codes:** (140.3380) Laser materials; (350.4238) Nanophotonics and photonic crystals.

---

## References and links

1. A. K. Geim and K. S. Novoselov, "The rise of graphene," *Nat. Mater.* **6**(3), 183–191 (2007).
2. J. E. Riggs, Z. X. Guo, D. L. Carroll, and Y. P. Sun, "Strong luminescence of solubilized carbon nanotubes," *J. Am. Chem. Soc.* **122**(24), 5879–5880 (2000).
3. L. Cao, X. Wang, M. J. Mezzani, F. S. Lu, H. F. Wang, P. G. Luo, Y. Lin, B. A. Harruff, L. M. Veca, D. Murray, S. Y. Xie, and Y. P. Sun, "Carbon dots for multiphoton bioimaging," *J. Am. Chem. Soc.* **129**(37), 11318–11319 (2007).
4. H. Peng and J. Travas-Sejdic, "Simple aqueous solution route to luminescent carbogenic dots from carbohydrates," *Chem. Mater.* **21**(23), 5563–5565 (2009).
5. C. H. Lui, K. F. Mak, J. Shan, and T. F. Heinz, "Ultrafast photoluminescence from graphene," *Phys. Rev. Lett.* **105**(12), 127404 (2010).
6. X. M. Wu, H. Q. Cao, B. J. Li, and G. Yin, "The synthesis and fluorescence quenching properties of well soluble hybrid graphene material covalently functionalized with indolizine," *Nanotechnology* **22**(7), 075202 (2011).
7. X. M. Sun, D. C. Luo, J. F. Liu, and D. G. Evans, "Monodisperse chemically modified graphene obtained by density gradient ultracentrifugal rate separation," *ACS Nano* **4**(6), 3381–3389 (2010).
8. G. X. Chen, M. H. Hong, T. C. Chong, H. I. Elim, G. H. Ma, and W. Ji, "Preparation of carbon nanoparticles with strong optical limiting properties by laser ablation in water," *J. Appl. Phys.* **95**(3), 1455–1459 (2004).
9. G. X. Chen, M. H. Hong, T. S. Ong, M. Lam, W. Z. Chen, H. I. Elim, W. Ji, and T. C. Chong, "Carbon nanoparticles based nonlinear optical liquid," *Carbon* **42**(12–13), 2735–2737 (2004).
10. X. Y. Li, H. Q. Wang, Y. Shimizu, A. Pyatenko, K. Kawaguchi, and N. Koshizaki, "Preparation of carbon quantum dots with tunable photoluminescence by rapid laser passivation in ordinary organic solvents," *Chem. Commun. (Camb.)* **47**(3), 932–934 (2010).
11. S. L. Hu, K. Y. Niu, J. Sun, J. Yang, N. Q. Zhao, and X. W. Du, "One-step synthesis of fluorescent carbon nanoparticles by laser irradiation," *J. Mater. Chem.* **19**(4), 484–488 (2009).
12. Y. P. Sun, B. Zhou, Y. Lin, W. Wang, K. A. Fernando, P. Pathak, M. J. Mezzani, B. A. Harruff, X. Wang, H. Wang, P. G. Luo, H. Yang, M. E. Kose, B. Chen, L. M. Veca, and S. Y. Xie, "Quantum-sized carbon dots for bright and colorful photoluminescence," *J. Am. Chem. Soc.* **128**(24), 7756–7757 (2006).
13. H. T. Li, X. D. He, Z. H. Kang, H. Huang, Y. Liu, J. Liu, S. Lian, C. H. Tsang, X. Yang, and S. T. Lee, "Water-soluble fluorescent carbon quantum dots and photocatalyst design," *Angew. Chem. Int. Ed. Engl.* **49**(26), 4430–4434 (2010).
14. J. Valenta, I. Pelant, and J. Linnros, "Waveguiding effects in the measurement of optical gain in a layer of Si nanocrystal," *Appl. Phys. Lett.* **81**(8), 1396–1398 (2002).

## 1. Introduction

Carbon nanostructures have attracted intensive research interests due to its superior properties of chemical stability, low toxicity and potential applications in photonics [1]. Since the first observation of photoluminescence (PL) from carbon nanotubes in 2000 [2], optical properties of carbon nanostructures are widely studied [3–9]. Different fabrication methods have been proposed to fabricate carbon nanostructures. For example, laser ablation method is commonly used to break graphite into carbon nanodots (C-dots) [10,11] with average diameter down to about 5 nm [12]. On the other hand, if the as-prepared C-dots have passivated with diamine-terminated oligomeric poly-(ethylene glycol), PL emission ranging from blue to red can be observed under different excitation energy. Chemical solution method, which has the capability to support multi-color emission and up-conversion luminescence, is also a simple approach to obtain carbon nanostructures [6,7]. C-dots fabricated by electrochemical method have demonstrated size-dependent PL and up-conversion radiations [13]. Nevertheless, mainly spontaneous emission was recorded from the previous PL measurement of carbon nanostructures. In this paper, we report our observation of room-temperature white-light amplified spontaneous from C-dots, which can be fabricated by laser irradiation method, under high-power laser excitation. Furthermore, optical gain per peak power of the C-dots dispersed inside N-Methylpyrrolidone (NMP) is found to be  $\sim 64 \text{ cm}^{-1} \text{ MW}^{-1}$  at the peak wavelength. This indicates that C-dots, which demonstrate population inversion under laser excitation at room temperature, can be a potential optical gain medium to realize wide-bandwidth light-emitting nanostructured devices.

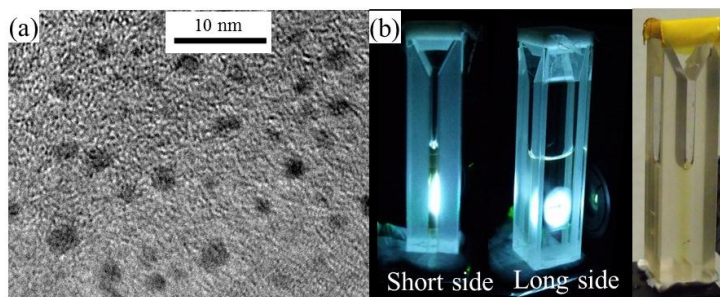


Fig. 1. (a) TEM images of C-dots, and (b) Photos of C-dots dispersed inside NMP.

## 2. Experimental methods and results

C-dots can be synthesized by a conventional laser irradiation method [11]. Graphite powder, which can be purchased from Fluka Analytical with size  $< 0.1 \text{ mm}$ , is used in the experiment. A 25 mg of the graphite powder is baked inside a furnace at  $100 \text{ }^\circ\text{C}$  for 1 hour in order to remove the moisture and to increase the solubility. Then, the graphite powder is poured into a glass macro-cell containing 1.5 mL of NMP. NMP, which is a transparent organic solvent and is highly compatible with multicyclocene particles, is chosen to disperse the graphite over the volume of the macro-cell. A Q-switched Nd:YAG (yttrium aluminum garnet) laser, which has a wavelength of 1064 nm and at pulsed operation ( $\sim 6 \text{ ns}$ , 10 Hz), is used to irradiate the black suspension (i.e., mixture of graphite powder and NMP). A laser beam, which has a diameter of 10 mm and a peak power density of  $\sim 100 \text{ MW/cm}^2$ , is irradiated onto the glass macro-cell. After 30 minutes of laser irradiation, a homogenous dark-brown transparent suspension can be observed from the macro-cell. The suspension is separated and removed from the macro-cell and then further diluted by NMP until the corresponding emission intensity is maximized under 266 nm laser excitation. It is noted that the high density of C-dots will result in fluorescence quenching and there is an optimized density of C-dots in NMP to obtain

maximum emission efficiency. This optimized density of C-dots in NMP is used throughout the experiment.

Figure 1(a) shows the transmission electron microscopy (TEM) image of the C-dots. A small portion of C-dot and NMP mixture is dropped onto a commercially available TEM grid. The measurement is performed after the NMP is completely evaporated from the TEM grid. From the TEM image, it is estimated that the size of C-dot is roughly varied between  $\sim 1.5$  and  $\sim 3.5$  nm. In order to measure the PL characteristics of the C-dot, the mixture is poured into a UV quartz micro-cell. Figure 1(b) shows a photo of the micro-cell filled with the mixture of C-dot and NMP. The mixture shows a uniform light-brown color, indicating that the C-dots should be uniformly distributed over the volume. Figure 1(b) also shows the photos of C-dots dispersed inside NMP under laser excitation by a quadruplet Q-switched Nd:YAG laser (at 266 nm) at pulsed operation ( $\sim 6$  ns, 10 Hz). A laser beam with a diameter of 1 cm is incident onto one side (with an internal width of 10 mm) of the micro-cell. It is observed that the mixture generates a very bright white-light emission.

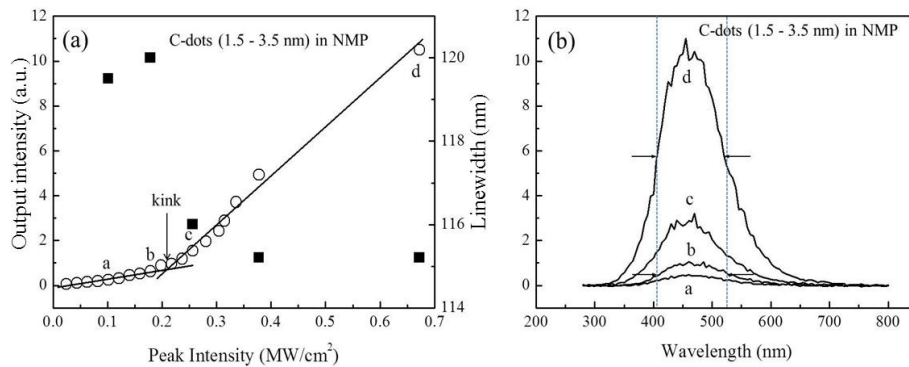


Fig. 2. (a) Plot of PL intensity as a function of excitation light intensity, and (b) FWHM of the emission spectra of the C-dots and NMP mixture under 266 nm laser excitation at room temperature.

Figure 2 shows a plot of light emission intensity as a function of light excitation intensity, or so-called light-light curve and emission spectra of the mixture measured under 266 nm laser excitation at room temperature. During the analysis, emission of the mixture is collected from the shorter side of the micro-cell with an internal width of 2 mm (i.e., perpendicular to the direction of the laser beam) through an objective lens and is coupled to an Oriel MS257 monochromator (spectral resolution of  $\sim 0.5$  nm) attached with a photo-multiplier tube. From the above plot, it is noted that there is a 'kink' occurs at an input intensity of  $\sim 0.21$  MW/cm<sup>2</sup>. Furthermore, peak wavelength and full-width at half-maximum (FWHM) of the emission spectra are found to be  $\sim 450$  and  $\sim 120$  nm respectively. The light emission may be due to the  $n \rightarrow \pi^*$  transition from the C = O bond of the carboxylic groups which are attached on the C-dots by C-C bonding. As the emission spectra cover a wide range of wavelength over the visible spectrum, it is not surprised that white-light emission can be observed from the mixture. In fact, it can be shown that the corresponding (x, y) coordinates on the CIE (commission on illumination) chromaticity diagram were found to be around (0.363, 0.356). Narrowing of the FWHM of the emission spectra from  $\sim 120$  to  $\sim 115$  nm was also recorded for the input intensities larger than the value of the 'kink' (i.e., for the input peak power density larger than  $\sim 0.21$  MW/cm<sup>2</sup>). Hence, the 'kink' observed from the light-light curve represents the pumping threshold of the mixture. In addition, the 'kink' represents the change of radiative process from spontaneous emission to amplified spontaneous emission.

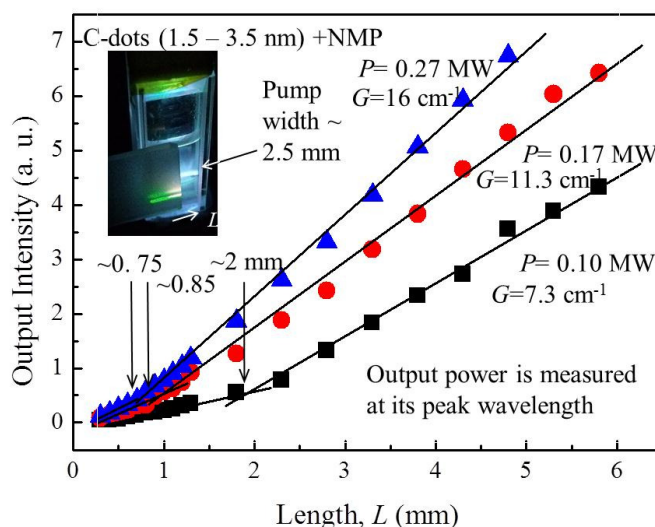


Fig. 3. Plot of output intensity versus pumping length  $L$  of the C-dots and NMP mixture for different pump intensities. The inset photo shows the experimental setup for the measurement.

Net optical gain of the C-dots dispersed inside the NMP can be measured by the variable stripe length (VSL) method. If  $L$  is the length of the pumping stripe and  $I_{tot}$  is the total intensity detected from the side of the micro-cell with an internal width of 2 mm, the corresponding net optical gain,  $G$ , can be obtained from the classical VSL equation as follows [14]:

$$I_{tot}(L, \lambda) = \frac{I_{sp}(\lambda)}{G(\lambda)} [\exp(G(\lambda)L) - 1] \quad (1)$$

where  $I_{sp}$  is the spontaneous emission intensity and  $\lambda$  is the wavelength of the net optical gain to be selected. Therefore, if the output intensity of the mixture at a particular  $\lambda$  is measured with different values of  $L$ , the corresponding  $G$  for some pump intensities can be deduced. In order to perform the calculation, the optical setup has been slightly modified. This can be done by using a cylindrical lens to focus a variable pumping stripe of maximum length and width equal to 10 and ~2.5 mm respectively onto the side of the micro-cell with an internal width of 10 mm, see the inset photo of Fig. 3. The pumping stripe is used in order to maintain the uniformity of the pumping intensity over the stripe region. Figure 3 also plots the room-temperature output intensity of the mixture at  $\lambda = \sim 450$  nm versus  $L$  for different pump intensities. It is observed that 'kinks' occur at around 2.0, 0.85 and 0.75 mm for pump power equal to 0.10, 0.17 and 0.27 MW respectively. The kinks represent the onset of the non-coherent optical feedback (i.e., light scattered by the C-dots). In fact, it can be shown that the light is weakly diffused inside the mixture due to the weak scattering strength of the C-dots. Therefore, the data recorded before the occurrence of the kink should be used to fit Eq. (1) for the estimation of  $G$ . It can be shown that the deduced value of  $G$  is 7.3, 11.3 and  $16 \text{ cm}^{-1}$  for input power equal to 0.10, 0.17 and 0.27 MW respectively. The optical gain per peak power of the mixture is estimated to be  $\sim 64 \text{ cm}^{-1} \text{ MW}^{-1}$ .

It is noted that NMP can emit visible radiation under ultraviolet excitation. Therefore, it is not sure whether the observed amplified spontaneous emission is from either C-dots or NMP. Hence, the emission characteristics of the NMP solution are also analyzed. Figure 4(a) plots the emission spectra of the NMP solution at different excitation intensities. It is noted that a dominant emission peak with peak wavelength at  $\sim 295$  nm is detected after the excitation of 266 nm light. Light-blue emission from the NMP can be observed from the naked eyes.

However, emission peak at  $\sim 295$  nm is not recorded from the emission spectra of the C-dots dispersed inside NMP, see Fig. 2(b). In addition, the emission intensity of NMP does not contribute much to the emission peak intensity of the mixture. This is because the emission intensity of NMP solution at around 450 nm is closed to the tail of its emission spectrum. The inset figure of Fig. 4(a) shows the light-light curve of the NMP solution. The light-light curve is a straight line which indicated that the emission obtained from the NMP solution is mainly spontaneous emission. These observations have verified that the NMP do not directly contribute to the white-light amplified spontaneous emission observed from the mixture and the  $\sim 295$  nm emission from the NMP solution may be re-absorbed by the C-dots. In fact, UV/vis absorption spectrum of C-dots has indicated that the C-dots have a strong absorption at around 300 nm, see Fig. 4(b). Hence, it is suspected that the emission intensity of C-dots dispersed inside the NMP is enhanced by the presence of NMP.

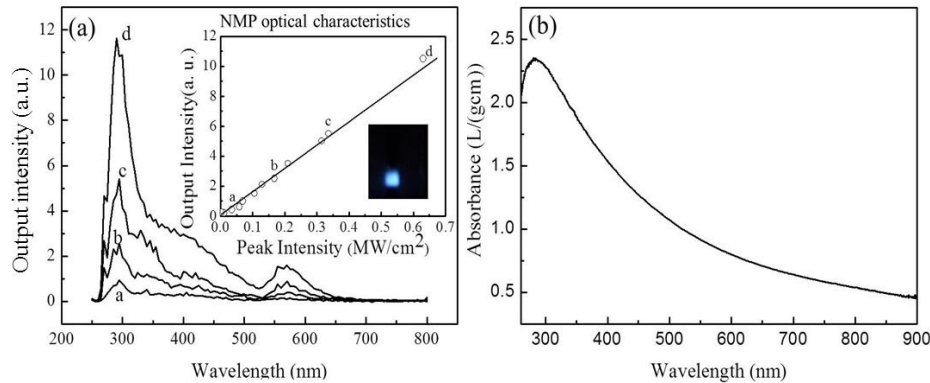


Fig. 4. (a) Plot of emission spectra of the NMP versus different pump intensities at room temperature. The inset shows the light-light curve and photo of the NMP under 266 nm laser excitation, and (b) Absorption spectrum of the C-dots.

Thin film of C-dots can be formed by evaporating the mixture on a quartz substrate so that the emission characteristics of the C-dots can be studied. Figure 5 plots the light-light curve and emission spectra of the C-dots thin film under laser excitation at room temperature. It is noted that the light-light curve has a kink at pump intensity equal to  $\sim 0.21$  MW/cm<sup>2</sup>. The image of the C-dots thin film under laser excitation is also shown in the inset of Fig. 5(b). Bright white-light emission can be clearly observed from the substrate. Furthermore, FWHM of the emission peaks, which have peak wavelength located at around 440 nm, reduces from  $\sim 200$  to  $\sim 175$  nm for the input intensity increase above the threshold. Hence, the C-dots thin film exhibits amplified spontaneous emission and the corresponding threshold value is close to that of the mixture. However, the emission intensity (FWHM of emission peaks) of C-dots thin film is lower (wider) than that of the mixture. These observations have confirmed that the presence of NMP enhances the optical-conversion efficiency of C-dots under laser excitation. This is because although a large portion of pump light has been scattered away and without being absorbed by the C-dots, the presence of NMP absorbs the remained pumping light and transfers the energy to the C-dots for the second time. As a result, the presence of NMP improves the emission intensity of C-dots and without affecting the emission characteristics. The optical gain per peak power of the C-dots can be estimated to be  $\sim 46$  cm<sup>-1</sup>MW<sup>-1</sup>. This implies that the presence of NMP can improve the optical gain per unit power of the C-dots by more than 39%.

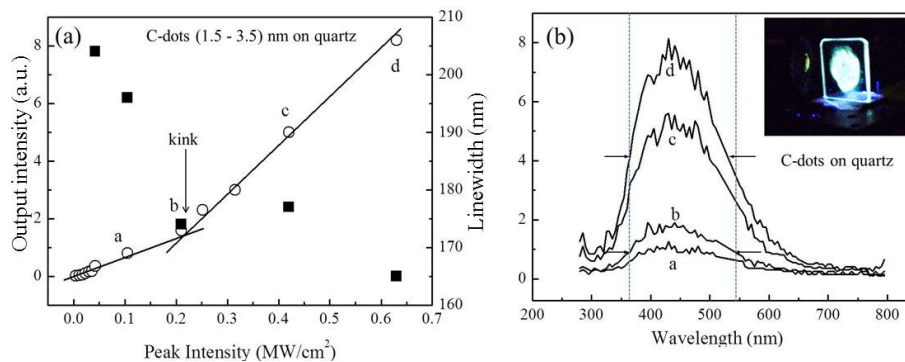


Fig. 5. (a) Plot of light–light curve and FWHM of the emission spectra of the C-dots deposited on a quartz substrate, and (b) The corresponding emission spectra. The inset shows the photo of C-dots on quartz substrate under laser excitation.

### 3. Conclusions

In summary, C-dots with diameter varies from ~1.5 to ~3.5 nm are fabricated by a conventional laser irradiation method. White-light amplified spontaneous emission is observed at room temperature for the C-dots under laser excitation at 266 nm. This is because the C-dots exhibit 1) a ‘kink’ from their light-light curve and 2) narrowing of FWHM of the emission peaks for pump intensity increase beyond the ‘kink’ position. For the C-dots uniformly dispersed inside NMP, it is found that the emission performance of the mixture can be improved – the optical gain per peak power increases by 39% to about  $\sim 64 \text{ cm}^{-1}\text{MW}^{-1}$  at the peak wavelength. The enhancement of emission efficiency of the C-dots with the presence of NMP is due to 1) the  $\sim 295 \text{ nm}$  emission from NMP after the excitation at 266 nm, and 2) the optical absorption of C-dots at  $\sim 295 \text{ nm}$ . Hence, the remained excitation light energy, which is not absorbed by the C-dots, is transferred indirectly to the C-dots via NMP. As a result, the optical gain per unit power of the C-dots can be improved by the NMP. The absorption and emission mechanism of NMP, however, do not affect the emission characteristics of the C-dots. Therefore, the results have indicated that the mixture may have potential applications as wide-bandwidth light-emitting nanostructured devices.

### Acknowledgments

This work was supported by the HK PolyU grants (Grant no. 1-ZV6X and G-YJ73).